A unique strategy for improving top contact in Si/ZnO hierarchical nanoheterostructure photodetectors

ARTICLE *in* CRYSTENGCOMM · APRIL 2012

Impact Factor: 4.03 · DOI: 10.1039/C2CE06715C

CrystEngComm

Cite this: *CrystEngComm*, 2012, **14**, 3015

www.rsc.org/crystengcomm

COMMUNICATION

A unique strategy for improving top contact in Si/ZnO hierarchical nanoheterostructure photodetectors

Wei Wang, Qing Zhao,* Jun Xu and Dapeng Yu*

Received 21st December 2011, Accepted 9th February 2012
DOI: 10.1039/c2ce06715c

Three-dimensional p-Si nanopillar/n-ZnO nanowire-array hierarchical nanoheterostructure photodetectors were achieved *via* a highly accessible and controllable fabrication process. By introducing PMMA to provide a flat, continuous and uniform surface, unique high transparency, low resistance top contact has been fabricated. The improved front electrode showed very small sheet resistivity of 0.002 Ω cm, two orders of magnitude lower than that of direct deposition of ITO onto ZnO (0.58 Ω cm).

Three-dimensional hierarchical nanoheterostructures offer direct heteroepitaxial nanoscale intergration of materials with different properties, which often leads to function intergration or novel applications. Moreover, such hierarchical nanoheterostructures offer greatly enhanced surface areas, which has attracted intensive research interest towards optoelectronic, photocatalysis, and photovoltaic applications.[1–8] In particular, ZnO is considered a promising material for photovoltaic devices due to it possessing a wide band gap (3.37 eV), large exciton binding energy (60 meV) and high photoconductivity gain.[9] On the other hand, Si nanopillars have been intensively investigated for the use in energy harvesting applications due to their unique optical and electrical properties.[10] Photodiodes based on p-Si nanowire/n-ZnO thin film heterojunction combinations have been reported recently, but the use of ZnO film on the top may increase light reflection and decrease the light harvest of the devices.[11,12] For this reason, a ZnO/Si hierarchical nanoheterostructure photodetector was fabricated by solution synthesis.[13] However, it still suffers from low energy conversion because of non-uniform top contact and recombination loss *via* defects. In fact, most 1D nanowire-array based photovoltaic devices suffer from poor top contact issues because fabricating a high light transmission and low resistance front electrode is very challenging. For example, direct deposition of a transparent conductive layer, such as ITO, onto the nanowire surface always leads to a high-resistivity top contact,[13–16] which will severely affect the device performance. Liquid top electrodes help to form a full contact with nanowires but result in low charge mobility and make the cell package rather difficult.[17,18] Therefore, developing a novel method to produce uniform top contact with low resistance is crucial in achieving high efficiency nanowire array-based photovoltaic devices.

Herein, three-dimensional p-Si nanopillar array/n-ZnO layer/n-ZnO nanowire array hierarchical heterostructure photodetectors were fabricated *via* a controllable method. Introducing the ZnO nanowire array on the top of the device enhanced light trapping and thus decreased light reflection. Most importantly, a high transparency, low resistivity top contact was achieved *via* a newly developed method. By creatively introducing PMMA onto the ZnO nanowire arrays and subsequent plasma etching, a uniform and continuous flat surface was supplied for the next ITO coating, which led to a front electrode resistance decrease by two orders of magnitude. Our results provide a general way to improve the top contact of nanowire array-based photovoltaic devices.

The schematic diagram of the fabrication of p-Si nanopillars/n-ZnO layer/n-ZnO nanowire array heterostructures is shown in Fig. 1. Wafer-scale Si nanopillar arrays (Fig. 1(a)) were obtained by a metal-assisted chemical etching process, as reported elsewhere.[16,19,20] Subsequently, ZnO nanowire arrays with a ZnO thin layer were deposited onto the Si nanopillars by chemical vapour deposition (CVD) (Fig. 1(b)).[21] The ZnO layer primarily tended to fill in the gap between the Si nanopillars and ZnO nanowire arrays. Briefly, a mixture of 0.15 g Zn powder and 0.05 g $AlCl_3$ powder, in a quartz tube, and a Si wafer, 2 cm downstream from the quartz tube, were placed in a furnace tube. The furnace was heated to and maintained at 700 °C, 10 Pa for 6 min with 100 sccm Ar and 8 sccm O_2. For the front electrode fabrication, PMMA (8%) mixed with anisole was spin coated (1000 rpm, 1 min) onto the top of the ZnO nanowires (Fig. 1(c)). This step provided a very flat, smooth and continuous surface and the PMMA completely covered the top of the ZnO nanowire arrays. Afterwards, part of the PMMA layer was plasma etched away (flow rate: 15 sccm, pressure: 10 Pa, power: 50 W for 30 s) to let the 150 nm–200 nm ZnO nanowire tips stand out from the PMMA surface, as Fig. 1(d) showed. Then a 150 nm–300 nm thick ITO film was sputtered onto the ZnO nanowire tips to make a good, continuous, and direct contact with the ZnO nanowires (Fig. 1(e)).

All surface morphology of the samples was characterized by scanning electron microscopy (SEM, FEI, NanoSEM 430). The spectral photoresponse and optical properties were measured by QTest Station 1000AD system (CrownTech Inc). The current density–voltage (*J–V*) characteristics were tested by a Keithley 4200SCS (Keithley Instruments, Inc) in the dark and under 1.5 a.m. solar simulator illumination (100 mW cm^{-2}, IVTest Station 2000,

State Key Laboratory for Mesoscopic Physics and Electron Microscopy Laboratory, School of Physics, Peking University, Beijing 100871, P. R. China. E-mail: zhaoqing@pku.edu.cn; yudp@pku.edu.cn

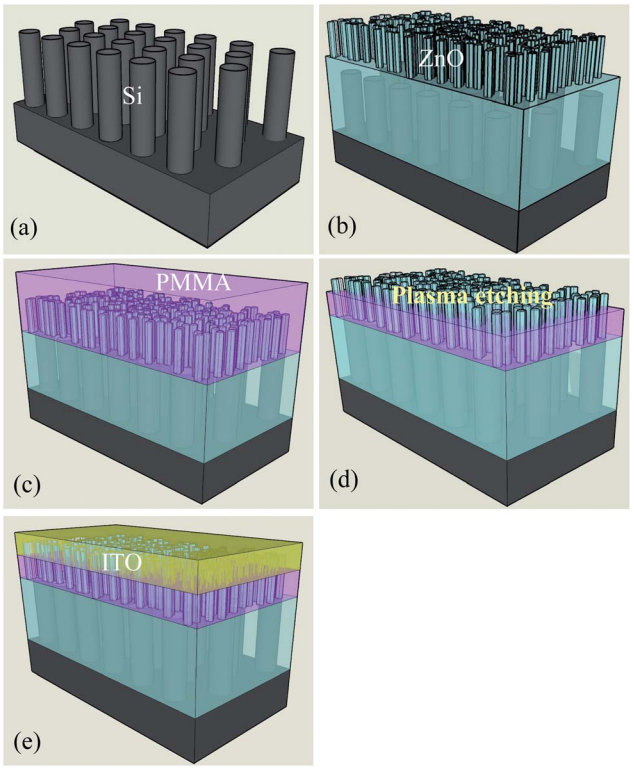

Fig. 1 Schematic diagram of the fabrication process for the Si/ZnO/PMMA/ITO devices. (a) Obtained a highly ordered Si nanopillar array by a metal-assisted chemical etching method. (b) Grew a ZnO layer and ZnO nanowire arrays onto Si nanopillar arrays. (c) Spin coated a PMMA layer onto the ZnO nanowire arrays. (d) Plasma etched part of the PMMA layer to let the ~150 nm ZnO nanowire tips stand out from the PMMA. (e) Deposited ITO film onto the exposed ZnO nanowire tips and PMMA layer.

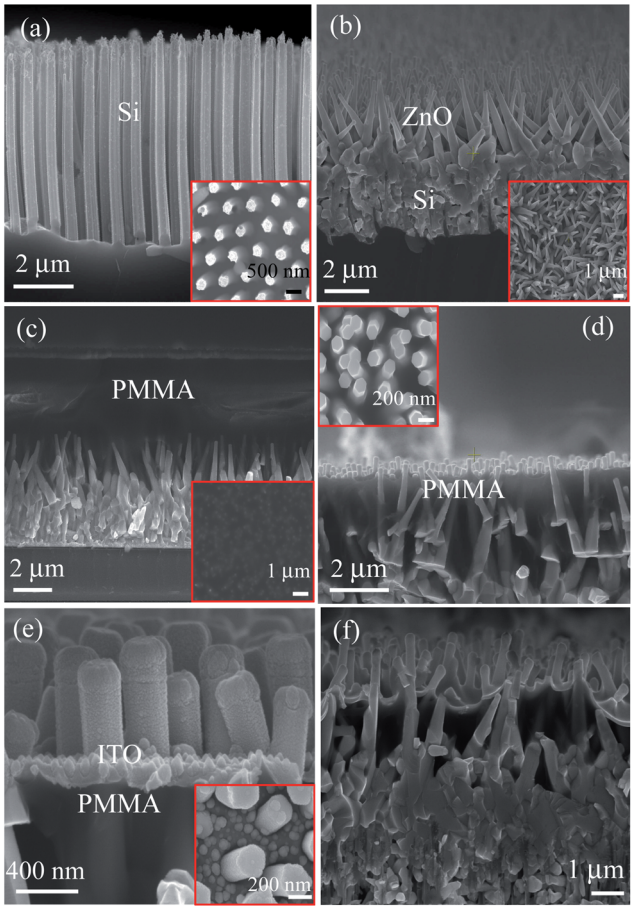

Fig. 2 Typical cross-section SEM images of the fabricated device in each step. Inset: corresponding top-view SEM images. (a) Highly ordered Si nanopillar arrays with a uniform filling ratio. (b) As-deposited ZnO layer and ZnO nanowire arrays onto the Si nanopillar arrays. (c) PMMA coating on the ZnO nanowires. (d) After plasma etching, the ZnO nanowire tips stood out from the supporting PMMA layer. (e) ITO deposition onto the ZnO nanowires and PMMA layer to form a continuous, direct and good contact with ZnO. (f) The as-fabricated Si/ZnO/PMMA/ITO device.

CrownTech. INC). The solar simulator was carefully calibrated before each measurement. More than 20 devices were tested and the average active area of the device was 1 cm^2. The sheet resistivity of different front electrodes was measured by a four-probe probe station (Keithley 4200SCS) by the collinear four-probe method.

Fig. 2(a) displays a typical morphologic SEM image of Si nanopillar arrays with a length of 4 μm and diameter of 300 nm. The length and diameter were purposely designed and achieved *via* a controllable method to tailor the absorption spectra according to previous reports.[22,23] Fig. 2a and its inset distinctly demonstrate that our Si nanopillar array is highly ordered with a uniform filling ratio. The highly oriented ZnO nanowire arrays (d: 500 nm, l : 2 μm) with a ZnO layer were grown on top of the Si nanopillar arrays with a very high density (Fig. 2(b)). The inset of Fig. 2(b) demonstrates the uniformity and high orientation of the as-grown ZnO nanowire arrays. Fig. 2(c) shows a cross-section SEM image of the ZnO nanowires after PMMA coating on the top, revealing that PMMA completely covered the ZnO nanowires and supplied a flat, uniform and continuous surface. After an air plasma etching process, the ZnO nanowire tips were clearly observed standing out from the PMMA supporting membrane beneath (Fig. 2(d)). Plasma etching could achieve a controllable thickness as PMMA can be etched away and a length of the ZnO nanowire tip can be exposed. The inset of Fig. 2(d) depicts the exposed ZnO nanowire tips standing out from the PMMA layer. After depositing the ITO film on top of the ZnO nanowire tips, a uniform, continuous, and direct ohm contact was achieved between ZnO and ITO (Fig. 2(e)). From the inset of Fig. 2(e), ITO has been uniformly deposited onto the ZnO nanowires and the PMMA layer underneath. A three-dimensional p-Si/n-ZnO nanowire array hierarchical heterostructure photodetector was fabricated, shown in the typical cross section SEM image in Fig. 2(f). PMMA is very important in this strategy because it provides a flat and continuous surface for further conductive ITO layer deposition. The contact between ITO and the ZnO nanowires has been significantly improved with PMMA as a supporting membrane underneath, which is more advantageous than direct deposition of ITO onto the ZnO nanowires without using PMMA. Since the ZnO nanowire surface is not flat, direct deposition of ITO onto the ZnO nanowires could lead to a discontinuous contact and very high resistivity. Sheet resistivity of ZnO/ITO and ZnO/PMMA/ITO front electrodes was measured and the results are summarized in Table 1. As can be seen, after integration of PMMA, top contact (ZnO/PMMA/ITO) has been remarkably improved with a significant decrease in resistivity, from 0.58 to 0.002 Ω cm, more than two orders of magnitude smaller than that of ZnO/ITO.

Table 1 Photovoltaic characteristics of the photodetectors with different front electrode types

Front electrode type	Sheet resistivity (Ω cm)	V_{oc} (mV)	J_{sc} (mA cm^{-2})	FF (%)	Efficiency (%)
ZnO/ITO	0.58	160	8.34	16.9	0.225
ZnO/PMMA/ITO	2.24×10^{-3}	256	11.50	17.0	0.512

Optical properties of each layer were measured and displayed in Fig. 3(a). PMMA has a very high transparency with very high transmission (90%) from 300–800 nm. The transmission spectra of ITO and PMMA indicate that most photons with a wavelength longer than 300 nm could reach the ZnO layer, implying that introducing PMMA does not depress the optical absorption of the devices. Transmission of ZnO shows that the ZnO layer offers good light transmission of most photons with a wavelength >460 nm. Profiting from the highly ordered Si nanopillar arrays, the Si layer has an extremely low reflection (<4%) over a wide spectral bandwidth from 400 to 800 nm. The reflection spectra of the entire fabricated device is also quite low (<10%), suggesting that the ZnO nanowire arrays on top of the device perform as light trapping sites to enhance light harvest.[13,24] The light reflection of the entire device is higher than that of Si nanopillar arrays, which may be because the as-grown ZnO nanowire arrays are not as well-aligned as the Si nanopillar arrays. Further ITO coating onto the ZnO nanowires may also affect the light reflection of the device. The unique structure of integration of the ZnO layer and ZnO nanowire arrays with highly ordered Si nanopillar arrays greatly reduced light reflection and enhanced light absorption in the photodetector devices.

The *I–V* characteristics of Si/ZnO/PMMA/ITO and Si/ZnO/ITO devices were characterized in the dark and under 1.5 a.m. solar simulator illumination at room temperature (Fig. 3(b)). Both dark and photocurrent density–voltage characteristics were rectifying. *J–V* characteristics of the device with a front electrode of ZnO/ITO and ZnO/PMMA/ITO are summarized in Table 1. As seen in Table 1, both the short circuit current density (J_{sc}) and the open circuit voltage (V_{oc}) have been dramatically increased after the great improvement in top contact. In detail, V_{oc} and J_{sc} have been increased from 160 to 256 mV and 8.34 to 11.5 mA cm^{-2}, respectively, almost a 60% and 40% increase for a ZnO/PMMA/ITO front electrode compared to ZnO/ITO electrodes. Although V_{oc} and J_{sc} can be affected by many parameters of a p–n junction device, here we only change the top contact fabrication and keep the other parameters the same. Therefore, the increase in V_{oc} and J_{sc} of the device can be reasonably attributed to the much-decreased sheet resistivity of the top electrode. The overall light conversion efficiency has been remarkably enhanced after the use of the significantly improved top contact. The entire device with a ZnO/PMMA/ITO top contact demonstrated a power conversion efficiency of $\eta = 0.512\%$, with J_{sc} of 11.5 mA cm^{-2}, V_{oc} of 256 mV, which show a greater improvement than the recently reported ZnO/Si hierarchical nanoheterostructures ($\eta = 0.154\%$, $J_{sc} = 4.1$ mA cm^{-2}, $V_{oc} = 150$ mV).[13] Shown in Table 1, the photovoltaic performance has been significantly improved after improving the top contact fabrication, indicating that our method of introducing PMMA as a supporting membrane for ITO deposition is very effective in increasing the light conversion efficiency in solar cell devices based on nanowire array structures.

The spectral photoresponse and incident photon-to-electron conversion efficiency (IPCE) of the Si/ZnO nanowire array nanoheterostructures were measured and are shown in Fig. 3(c). The responsivity was kept at a high value of ~0.3 A W^{-1} in a wide wavelength range (400–1000 nm) and the maximum was as high as 0.4 A W^{-1} at around 800 nm. IPCE has a high value around 25% in a wide wavelength range from 400–1000 nm, owing to efficient light

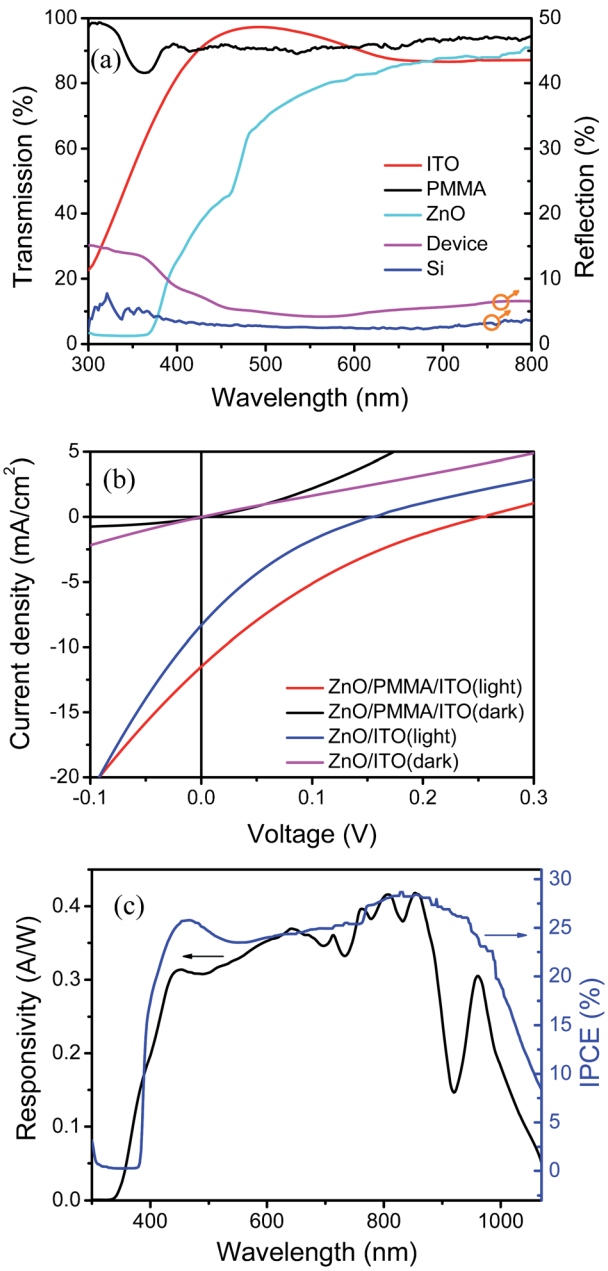

Fig. 3 (a) Transmission spectra of ITO, PMMA, the ZnO layer and the reflection spectra of the Si layer and the device. (b) *J–V* curve, in the dark and under illumination, with different front electrodes. (c) Spectral photoresponsivity and IPCE of Si/ZnO nanowire heterostructure devices from 300 to 1100 nm.

absorption of the ZnO and Si layer. The as-designed Si/ZnO nanoheterostructure devices make efficient use of light and have a significantly improved IPCE, much larger than the recently reported value (2.2%) from a Si/ZnO hierarchical nanoheterostructure.[13] There are several ways to improve the performance of the Si/ZnO nanoheterostructure devices, such as interface treatment to make better contact between Si and ZnO; increasing carrier concentration by proper ZnO doping; optimization of Si nanopillar length, *etc.*

In summary, three-dimensional p-Si nanopillar/n-ZnO layer/ZnO nanowire array hierarchical heterostructure photodetectors were fabricated *via* a controllable method. The unique combination of Si nanopillars with a ZnO layer and ZnO nanowire arrays demonstrated an enhanced light-trapping effect due to the arranged nanowire arrays and high reflective index material filling. More importantly, the unique strategy of using PMMA as a void-filling material to obtain a continuous, uniform and low-resistance front electrode has greatly decreased the top contact resistivity by two orders of magnitude. As a result, the overall device shows a peak photoresponsivity of 0.4 A W^{-1} at ~800 nm. Our results provide a very effective and versatile approach to dramatically improve the top contact of photovoltaic devices based on 1D nanowire/nanopillar array structures.

Acknowledgements

This project is financially supported by the National Natural Science Foundation of China (NSFC 50902004, 11023003, 10974003), and National 973 projects (No. 2009CB623703, 2011CB707600, MOST) from China's Ministry of Science and Technology. We acknowledge the International Science & Technology Cooperation Program of China, Sino Swiss Science and Technology Cooperation Program (2010DFA01810) and FP7 EU IRSES project (MICROCARE) No. 247641.

References

1 Z. Y. Fan, D. J. Ruebusch, A. A. Rathore, R. Kapadia, O. Ergen, P. W. Leu and A. Javey, *Nano Res.*, 2009, **2**, 829–843.
2 Y. Huang, X. F. Duan, Q. Q. Wei and C. M. Lieber, *Science*, 2001, **291**, 630–633.
3 M. C. McAlpine, R. S. Friedman, S. Jin, K. H. Lin, W. U. Wang and C. M. Lieber, *Nano Lett.*, 2003, **3**, 1531–1535.
4 S. E. Han and G. Chen, *Nano Lett.*, 2010, **10**, 1012–1015.
5 Z. Y. Fan, H. Razavi, J. W. Do, A. Moriwaki, O. Ergen, Y. L. Chueh, P. W. Leu, J. C. Ho, T. Takahashi, L. A. Reichertz, S. Neale, K. Yu, M. Wu, J. W. Ager and A. Javey, *Nat. Mater.*, 2009, **8**, 648–653.
6 S. A. McDonald, G. Konstantatos, S. Zhang, P. W. Cyr, E. J. D. Klem, L. Levina and E. H. Sargent, *Nat. Mater.*, 2005, **4**, 138–142.
7 S. H. Ko, D. Lee, H. W. Kang, K. H. Nam, J. Y. Yeo, S. J. Hong, C. P. Grigoropoulos and H. J. Sung, *Nano Lett.*, 2011, **11**, 666–671.
8 O. L. Muskens, J. G. Rivas, R. E. Algra, E. P. A. M. Bakkers and A. Lagendijk, *Nano Lett.*, 2008, **8**, 2638–2642.
9 Q. Zhang, C. S. Dandeneau, X. Zhou and G. Cao, *Adv. Mater.*, 2009, **21**, 4087–4108.
10 K. Q. Peng and S. T. Lee, *Adv. Mater.*, 2011, **23**, 198–215.
11 C.-Y. Huang, Y.-J. Yang, J.-Y. Chen, C.-H. Wang, Y.-F. Chen, L.-S. Hong, C.-S. Liu and C.-Y. Wu, *Appl. Phys. Lett.*, 2010, **97**, 013503.
12 H.-D. Um, S. A. Moiz, K.-T. Park, J.-Y. Jung, S.-W. Jee, C. H. Ahn, D. C. Kim, H. K. Cho, D.-W. Kim and J.-H. Lee, *Appl. Phys. Lett.*, 2011, **98**, 033102.
13 K. Sun, Y. Jing, N. Park, C. Li, Y. Bando and D. L. Wang, *J. Am. Chem. Soc.*, 2010, **132**, 15465–15467.
14 J.-Y. Wang, C.-Y. Lee, Y.-T. Chen, C.-T. Chen, Y.-L. Chen, C.-F. Lin and Y.-F. Chen, *Appl. Phys. Lett.*, 2009, **95**, 131117.
15 E. C. Garnett and P. Yang, *J. Am. Chem. Soc.*, 2008, **130**, 9224–9225.
16 K. Peng, Y. Xu, Y. Wu, Y. Yan, S.-T. Lee and J. Zhu, *Small*, 2005, **1**, 1062–1067.
17 K.-Q. Peng, X. Wang, X. Wu and S.-T. Lee, *Appl. Phys. Lett.*, 2009, **95**, 143119.
18 Y. Wei, C. Xu, S. Xu, C. Li, W. Wu and Z. L. Wang, *Nano Lett.*, 2010, **10**, 2092–2096.
19 D. F. Liu, Y. J. Xiang, X. C. Wu, Z. X. Zhang, L. F. Liu, L. Song, X. W. Zhao, S. D. Luo, W. J. Ma, J. Shen, W. Y. Zhou, G. Wang, C. Y. Wang and S. S. Xie, *Nano Lett.*, 2006, **6**, 2375–2378.
20 Z. Huang, H. Fang and J. Zhu, *Adv. Mater.*, 2007, **19**, 744–748.
21 Y. C. Kong, D. P. Yu, B. Zhang, W. Fang and S. Q. Feng, *Appl. Phys. Lett.*, 2001, **78**, 407.
22 L. Hu and G. Chen, *Nano Lett.*, 2007, **7**, 3249–3252.
23 J. S. Li, H. Y. Yu, S. M. Wong, G. Zhang, X. W. Sun, P. G. Q. Lo and D. L. Kwong, *Appl. Phys. Lett.*, 2009, **95**, 033102.
24 C. Battaglia, J. Escarré, K. Söderström, L. Erni, L. Ding, G. g. Bugnon, A. Billet, M. Boccard, L. Barraud, S. De Wolf, F.-J. Haug, M. Despeisse and C. Ballif, *Nano Lett.*, 2011, **11**, 661–665.

